J Neuropathol Exp Neurol
Vol. 76, No. 7, July 2017, pp. 605–619
doi: 10.1093/jnen/nlx041

ORIGINAL ARTICLE

Multisite Assessment of Aging-Related Tau Astrogliopathy (ARTAG)

Gabor G. Kovacs, MD, PhD, Sharon X. Xie, PhD, Edward B. Lee, MD, PhD, John L. Robinson, BA, Carrie Caswell, MS, David J. Irwin, MD, PhD, Jon B. Toledo, MD, PhD, Victoria E. Johnson, MD, Douglas H. Smith, MD, Irina Alafuzoff, MD, PhD, Johannes Attems, MD, Janos Bencze, MD, Kevin F. Bieniek, PhD, Eileen H. Bigio, MD, Istvan Bodi, MD, Herbert Budka, MD, Dennis W. Dickson, MD, Brittany N. Dugger, PhD, Charles Duyckaerts, MD, Isidro Ferrer, MD, Shelley L. Forrest, PhD, Ellen Gelpi, MD, Stephen M. Gentleman, PhD, Giorgio Giaccone, MD, Lea T. Grinberg, MD, Glenda M. Halliday, PhD, Kimmo J. Hatanpaa, MD, Patrick R. Hof, MD, Monika Hofer, MD, Tibor Hortobágyi, MD, PhD, James W. Ironside, FRCPath, Andrew King, FRCPath, Julia Kofler, MD, Enikö Kövari, MD, Jillian J. Kril, PhD, FFSc, Seth Love, FRCPath, Ian R. Mackenzie, MD, Qinwen Mao, MD, PhD, Radoslav Matej, MD, PhD, Catriona McLean, MBBS, MD, David G. Munoz, MD, Melissa E. Murray, PhD, Janna Neltner, MD, Peter T. Nelson, MD, Diane Ritchie, PhD, Roberta D. Rodriguez, MD, PhD, Zdenek Rohan, MD, PhD, Annemieke Rozemuller, MD, PhD, Kenji Sakai, MD, Christian Schultz, MD, Danielle Seilhean, MD, PhD, Vanessa Smith, MD, Pawel Tacik, MD, Hitoshi Takahashi, MD, Masaki Takao, MD, Dietmar Rudolf Thal, MD, PhD, Serge Weis, MD, PhD, Stephen B. Wharton, FRCPath, Charles L. White III, MD, John M. Woulfe, MD, Masahito Yamada, MD, PhD, and John Q. Trojanowski, MD, PhD

Abstract

Aging-related tau astrogliopathy (ARTAG) is a recently introduced terminology. To facilitate the consistent identification of ARTAG and to distinguish it from astroglial tau pathologies observed in the primary frontotemporal lobar degeneration tauopathies we evaluated how consistently neuropathologists recognize (1) different astroglial tau immunoreactivities, including those of ARTAG and those associated with primary tauopathies (Study 1); (2) ARTAG types (Study 2A); and (3) ARTAG severity (Study 2B). Microphotographs and scanned sections immunostained for phosphorylated tau (AT8) were made available for download and preview. Percentage of agreement and kappa values with 95% confidence interval (CI) were calculated for each evaluation. The overall agreement for Study 1 was >60% with a kappa value of 0.55 (95% CI 0.433–0.645). Moderate agreement (>90%, kappa 0.48, 95% CI 0.457–0.900) was reached in Study 2A for the identification of ARTAG pathology for each ARTAG subtype (kappa 0.37–0.72), whereas fair agreement (kappa 0.40, 95% CI 0.341–0.445) was reached for the evaluation of ARTAG severity. The overall assessment of ARTAG showed moderate agreement (kappa 0.60, 95% CI 0.534–0.653) among raters. Our study supports the application of the current harmonized evaluation strategy for ARTAG with a slight modification of the evaluation of its severity.

Key Words: Aging, ARTAG, Digital pathology, Interrater agreement, Neuropathology, Tau, Tau-astrogliopathy.

From the Institute of Neurology, Medical University of Vienna (GGK, HB), Vienna, Austria; Center for Neurodegenerative Disease Research, Institute on Aging and Department of Pathology and Laboratory Medicine of the Perelman School of Medicine at the University of Pennsylvania (GGK, EBL, JLR, DJI, JBT, JQT); and Department of Biostatistics and Epidemiology (SXX, CC); and Department of Neurosurgery, Center for Brain Injury and Repair, University of Pennsylvania (VEJ, DHS), Philadelphia, Pennsylvania; Department of Immunology, Genetics and Pathology, Uppsala University (IA), Uppsala, Sweden; Institute of Neuroscience, Newcastle University (JA), Newcastle upon Tyne, UK; Department of Neuropathology, Institute of Pathology, Faculty of Medicine, University of Debrecen (JB, TH), Debrecen, Hungary; Department of Neuroscience, Mayo Clinic (KFB, DWD, MEM, PT), Jacksonville, Florida; Northwestern University Feinberg School of Medicine, Northwestern ADC Neuropathology Core (EHB, QM), Chicago, Illinois; Clinical Neuropathology, King's College Hospital and London Neurodegenerative Brain Bank (IB, AK), London, UK; Institute of Neuropathology, University Hospital Zurich (HB), Zurich, Switzerland; University of California San Francisco, Institute for Neurodegenerative Diseases (BND), San Francisco, California; Neuropathology Department, Hôpital de La Salpetrière, AP-HP, UPMC-Sorbonne-University (CD, DS), Paris, France; Institute of Neuropathology, Bellvitge University Hospital, University of Barcelona (IF), CIBERNED, Hospitalet de Llobregat, Barcelona, Spain; Discipline of Pathology, Sydney Medical School, The University of Sydney (SLF, JJK), Sydney, Australia; Neurological Tissue Bank of the Biobank-Hospital Clinic-IDIBAPS, Institut d'Investigacions Biomediques Pi i (EG), Barcelona, Spain; Department of Medicine, Imperial College London (SMG), London, UK; IRCCS Foundation "Carlo Besta" Neurological Institute (GG), Milan, Italy; Memory and Aging Center, Department of Neurology, University of California (LTG), San Francisco, California; Department of Pathology,

INTRODUCTION

Neuropathological assessment of neurodegenerative conditions and brain aging is witnessing a renaissance. New body fluids and neuroimaging biomarkers are being identified, the evaluation and validation of which require diagnostic certainty established by neuropathological assessment (1). New disease concepts and diagnostic criteria have emerged. In 2012, the National Institute on Aging (NIA) in collaboration with the Alzheimer's Association (AA) revised consensus guidelines for the neuropathological assessment of Alzheimer disease (AD) (2). AD neuropathological evaluation yielded data that show a high level of agreement with potential modifications for modest improvements (3). The concept of primary age-related tauopathy (PART) was published, providing an evaluation and interpretation of neurofibrillary tangle pathology in the medial temporal lobe (4). Although pathological accumulation of abnormally phosphorylated tau protein in astrocytes has been frequently noted in the brains of elderly individuals (5–7), there has been no consensus on how to describe these findings. In addition, clinicians and biomarker researchers were largely unaware of this type of astroglial tau pathology. To stimulate clinicopathological studies and research into the pathobiology of astrocytic tau pathology, an international group of neuropathologists and researchers published a strategy for the harmonized consensus evaluation of aging-related tau astrogliopathy (ARTAG) (8). This strategy includes 4 steps in the assessment of ARTAG: i) identification of subpial, subependymal, perivascular, and white and gray matter types of ARTAG; ii) documentation of regional involvement such as medial temporal lobe, lobar, subcortical, or brainstem; iii) description of subregional involvement; and iv) documentation of the severity of ARTAG (8).

Interlaboratory studies of the BrainNet Europe Consortium to evaluate the reproducibility of the assessments of various neuropathological variables have shown that multiple factors predispose to inconsistencies, including different fixation or staining methods (9), but also differences in the interpretation of immunoreactive features or staging systems (10–14). Therefore, evaluation of the reproducibility of consensus guidelines is an imperative prerequisite for the implementation of such guidelines.

The spectrum of astroglial tau pathologies extends beyond ARTAG and comprises various morphologies thought to be characteristic of so-called primary frontotemporal lobar

University of Sao Paulo Medical School (LTG), LIM, São Paulo, Brazil; Brain & Mind Centre, Sydney Medical School, The University of Sydney, and UNSW Medicine & NeuRA (GMH), Sydney, Australia; Department of Pathology, University of Texas Southwestern Medical Center (KJH, CLW), Dallas, Texas; Fishberg Department of Neuroscience, Friedman Brain Institute, and Ronald M. Loeb Center for Alzheimer's Disease, Icahn School of Medicine at Mount Sinai (PRH), New York, New York; Department of Neuropathology, John Radcliffe Hospital (MH), Oxford, UK; Centre for Clinical Brain Sciences, University of Edinburgh (JWI, DR), Edinburgh, UK; Department of Pathology, University of Pittsburgh (JK), Pittsburgh, Pennsylvania; Department of Mental Health and Psychiatry, University Hospitals and University of Geneva School of Medicine (EK), Geneva, Switzerland; Institute of Clinical Neurosciences, University of Bristol, Learning & Research Level 2, Southmead Hospital (SL), Bristol, UK; Department of Pathology and Laboratory Medicine, University of British Columbia (IRM), Vancouver, Canada; Department of Pathology and Molecular Medicine, Thomayer Hospital (RM, ZR), Prague, Czech Republic; Department of Pathology, First Medical Faculty, Charles University (RM, ZR), Prague, Czech Republic; Department of Anatomical Pathology, Alfred Hospital (CM), Prahran, Victoria, Australia; Division of Pathology, St. Michael's Hospital (DGM), Toronto, Ontario, Canada; Department of Pathology and Sanders-Brown Center on Aging, University of Kentucky (JN, PTN, VS), Lexington, Kentucky; Physiopathology in Aging Lab/Brazilian Aging Brain Study Group-LIM22, University of Sao Paulo Medical School (RDR), Sao Paulo, Brazil; Behavioral and Cognitive Neurology Unit, Department of Neurology, University of São Paulo (RDR), São Paulo, Brazil; Netherlands Brainbank, Amsterdam and Department of Pathology, VU University Medical Center (AR), Amsterdam, The Netherlands; Department of Neurology and Neurobiology of Aging, Kanazawa University Graduate School of Medical Sciences (KS, MY), Kanazawa, Japan; Institute of Neuroanatomy, Centre for Biomedicine and Medical Technology Mannheim, Medical Faculty Mannheim, Heidelberg University (CS), Heidelberg, Germany; Department of Neurodegenerative Diseases and Gerontopsychiatry at the University of Bonn Medical Center (PT), Bonn, Germany; Department of Pathology, Brain Research Institute, Niigata University (HT), Niigata, Japan; Department of Neurology, Saitama Medical University International Medical Center (MT), Saitama, Japan; Department of Neuroscience, Katholieke Universiteit-Leuven (DRT); and Department of Pathology, Universitaire Ziekenhuizen-Leuven (DRT), Leuven, Belgium; Laboratory of Neuropathology, Department of Pathology and Neuropathology, Kepler University Hospital, Medical School, Johannes Kepler University (SW), Linz, Austria; Sheffield Institute for Translational Neuroscience, University of Sheffield (SBW), Sheffield, UK; and Department of Pathology and Laboratory Medicine, Centre for Cancer Therapeutics, Ottawa Hospital Research Institute, University of Ottawa (JMW), Ontario, Canada.

Send correspondence to: Gabor G. Kovacs, MD, PhD, Institute of Neurology, Medical University of Vienna, AKH 4J, Währinger Gürtel 18-20, 1097 Vienna, Austria; E-mail: gabor.kovacs@meduniwien.ac.at and John Q. Trojanowski, MD, PhD, Department of Pathology and Laboratory Medicine, Center for Neurodegenerative Disease Research, Institute on Aging, University of Pennsylvania School of Medicine, HUP Maloney 3rd Floor, 36th and Spruce Streets, Philadelphia, PA 19104. E-mail: trojanow@mail.med.upenn.edu

Support for this work was provided by grants from the National Institute on Aging of the National Institutes of Health (P30 AG010124, P01 AG017586, P50 AG005138; NS088341 and NS094003). We also thank members of the Center for Neurodegenerative Disease Research at the University of Pennsylvania, Philadelphia, PA who contributed to this work, and the many patients studied and their families, for making the research reported here possible. PT is supported by an Allergan Medical Educational Grant, a Jaye F. and Betty F. Dyer Foundation Fellowship in progressive supranuclear palsy research, and a Max Kade Foundation postdoctoral fellowship. RM and ZR are supported by Charles University in Prague (Project Progres-Q28/LF1) and OPPK (Project CZ.2.16/3.1.00/24509). The National Brain Research Program, Hungary (KTIA_13_-NAP-A-II/7), supported TH. The Alzheimer's Australia Dementia Research Foundation via the Rosemary Foundation Travel Fellowship supports SLF and JJK. JK is supported by the ADRC NIH P50 AG005133 grant. GH is supported by the National Health & Medical Research Council of Australia Senior Principal Research Fellowship (1079679).

Dietmar Rudolf Thal received consultancies from Covance Laboratories (UK) and GE-Healthcare (UK) and has received a speaker honorarium from GE-Healthcare (UK) and collaborated with Novartis Pharma Basel (Switzerland). The other authors report no conflict of interest.

Supplementary Data can be found at http://www.jnen.oxfordjournals.org.

TABLE 1. Clinicopathological Data of the Cases Included in Study 1 (Evaluation of Photos) and Study 2A and 2B (Evaluation of Scanned Sections)

Case Nr.	Age	Sex	Neuropathology										Photo Number and Region					Scan Number and Region						
			AD/ PART	Braak Stage	Thal Phase	CERAD Score	AGD	ARTAG	PSP	CBD	GGT	Pick's Disease	Frontal Cx	Temporal Cx	Hippocampus	Amygdala	Basal Ganglia	Frontal Cx	Temporal Cx	Ant. cingulate	Hippocampus	Amygdala	Basal ganglia	Mesencephalon	Medulla obl.
Case-1	80	f	+	3	1	1	+	+	−	−	−	−		1					1						
Case-2	85	f	+	2	1	1	−	+	−	−	−	−		2–5			6–10	3	2				4	5	6
Case-3	87	f	+	3	1	1	−	+	−	−	−	−				11,12						7			
Case-4	89	f	+	3	2	1	+	+	−	−	−	−				13,14						8			
Case-5	83	f	+	6	5	3	+	+	+*	−	−	−					15,16						9		
Case-6	83	f	+	3	2	2	+	+	−	−	−	−		17–19							10				
Case-7	85	m	+	2	1	1	+	+	−	−	−	−				20						11			
Case-8	77	m	+	3	2	2	+	+	−	−	−	−			21				12					25	
Case-9	82	m	+	5	3	2	+	+	+	−	−	−			22						13				
Case-10	86	m	+	5	3	3	+	+	−	−	−	−			23						14				
Case-11	82	m	+	3	1	1	+	+	−	−	−	−	24					17							
Case-12	79	m	+	4	3	2	−	−	−	+	−	−		25, 28, 30					16						
Case-13	76	f	+	2	0	0	−	+†	+	−	−	−		26,27,29					19						
Case-14	88	f	+	4	3	3	+	+	−	−	−	−	31					22							
Case-15	63	f	−	−	−	−	−	−	−	−	+	−	32,34												
Case-16	55	m	−	−	−	−	−	−	−	−	−	+		33											
Case-17	65	f	−	−	−	−	−	−	−	−	−	+		35											
Case-18	82	f	+	2	1	1	−	+	−	−	−	−									15				
Case-19	87	f	+	3	0	0	+	+	+*	−	−	−								18			23		
Case-20	85	m	+	1	0	0	−	+	−	−	−	−									20				
Case-21	81	m	+	1	0	0	−	+†	−	−	−	−							21						
Case-22	83	m	+	2	1	1	+	+	−	−	−	−											24		

m, male; f, female; CERAD, Consortium to Establish a Registry for Alzheimer Disease; Cx, cortex. Braak stage refers to neurofibrillary degeneration (34) and Thal phase to Aβ deposition (35).

*Indicates that presence of subcortical neurofibrillary tangles were suggestive of early form of PSP.

†Indicates that ARTAG was represented by occasional GFA.

TABLE 2. Summary of Kappa Values (±95% Confidence Interval, CI) and Mean % of Agreement (±95% CI) for Different Aspects of Study 1 and 2

Study and Question	Kappa Value	95% CI	Mean % of Agreement	95% CI
1: Recognition of astrocytic tau immunoreactivities	0.55	0.433–0.645	63.8	±7.5
2A: Recognition of presence of ARTAG	0.48	0.457–0.900	91.1	±5.1
2A: Recognition of astrocytic tau immunoreactivities associated with FTLD-tau	0.25	$2.89x10^{-16}$–0.374	73.1	±6.3
2A: Recognition of SP ARTAG	0.61	0.468–0.739	81.8	±7.02
2A: Recognition of SE ARTAG	0.72	0.584–0.828	87.2	±5.9
2A: Recognition of GM ARTAG	0.37	0.288–0.536	83.1	±5.6
2A: Recognition of WM ARTAG	0.44	0.323–0.551	79.5	±6.05
2A: Recognition of PV ARTAG	0.58	0.442–0.672	78.1	±6.4
2B: Semiquantitative scoring	0.40	0.341–0.445	50.4 (65.9)	±3.8 (4.6)
2A+B: Overall assessment of ARTAG	0.60	0.534–0.650	82.3	±2.4

SP, subpial; SE, subependymal; GM, gray matter; WM, white matter; PV, perivascular.

degeneration (FTLD) tauopathies (FTLD-Tau) (15, 16). Accordingly, tufted astrocytes are associated with progressive supranuclear palsy (PSP) (17, 18), astrocytic plaques with corticobasal degeneration (CBD) (18, 19), globular astroglial inclusions with globular glial tauopathies (GGT) (20), and ramified astrocytes with Pick disease (PiD) (21). Most of these pathologies were initially defined using silver staining and later by immunohistochemical studies with antibodies specific for different modifications of the tau protein (22). In ARTAG, 2 astroglial tau-immunoreactive features have been recognized: thorn-shaped astrocytes (TSA) and granular/fuzzy astrocytes (GFA) (8). The bushy astrocytes reported in argyrophilic grain disease (AGD) (23) were included in the morphological spectrum of GFAs. In view of the lack of studies on how consistently neuropathologists can recognize patterns of astrocytic tau immunoreactivity in primary FTLD-Tau disorders including ARTAG, we set up a study to evaluate neuropathological recognition of i) different astroglial tau immunoreactivities including those of ARTAG and those associated with primary tauopathies; ii) ARTAG types; and iii) ARTAG severity. The primary aim of this study was to facilitate the consistent identification of ARTAG and to distinguish ARTAG from the astroglial tau pathologies related to primary FTLD-Tau.

MATERIALS AND METHODS

Case Selection and Evaluation

For this study, 22 cases were selected from the Brain Bank of the Institute of Neurology, Medical University of Vienna. Cases with PSP, CBD, PiD, GGT, and combined age-related pathologies (e.g. ARTAG, PART, AD, and AGD) were included. The cases of combined age-related pathologies were selected from the ongoing longitudinal VITA (Vienna Transdanubian Aging) study (7). Neuropathological data for the cases included in the study are summarized in Table 1. The same cases were used for Studies 1, 2A, and 2B (see below).

For Study 1, 35 digital microphotographs (400× magnification; 15× 11.3 cm width at 300 dpi) illustrating patterns of astrocytic tau immunoreactivity (antitau AT8; pS202/pT205, 1:200, Pierce Biotechnology, Rockford, IL) were provided from a total of 17 cases (Table 1). For each example, evaluators were asked to assign one of 6 different tau-morphologies (including tufted astrocyte, astrocytic plaque, globular astroglial inclusion, ramified astrocyte, GFA, and TSA) or as a seventh option "none of these." Participants were asked to rank their choice with a number "1" and, if it was unclear, were offered the option to indicate an alternative choice with a number "2."

In addition, a set of AT8-immunostained sections were scanned with a Pannoramic FLASH III digital slide scanner (3DHistech, Budapest, Hungary) (Study 2A and 2B) and made available as whole slide digital images for analysis with Pannoramic Viewer and Case Viewer 2.0 software (version 1.15-4) after download from the company's website (http://www.3dhistech.com/pannoramic_viewer, courtesy of 3DHistech, Budapest, Hungary) for the participants of the study. The microphotographs and whole slide digital images were evaluated alone (in total 42) or in small groups (in total 3) of 2–3 neuropathologists representing the institutions involved in the study. Overall 25 AT8-immunostained slides were scanned from 19 cases (Table 1). The digital slide viewer application, suitable for Windows and MacOs systems, was used to view the images. The sections represented different ARTAG subtypes showing different degrees of severity, and sections from primary tauopathy cases had also been included. In addition to detailed instructions, a separate Excel sheet was provided for each case (Supplementary Data S1 and S2). For gray and white matter, ARTAG-specific anatomical regions were submitted for evaluation. The evaluators had to i) decide whether ARTAG was present (yes/no); ii) indicate which type of ARTAG was present (yes/no question for each type); iii) indicate for each ARTAG type visible on the section whether the severity/extent was occasional or numerous; iv) indicate for each ARTAG type visible in the section, if numerous whether focally accentuated or widespread; and v) indicate whether other nonARTAG type of astroglial tau immunoreactivity was seen in the section or not (yes/no).

Observers at the different sites were blind to the "gold standard" neuropathological diagnosis of each case. Examples of the different forms of ARTAG and astrocytic tau immunoreactivities as well as a table summarizing the key features of each type of pathology were provided based on ARTAG's recent description

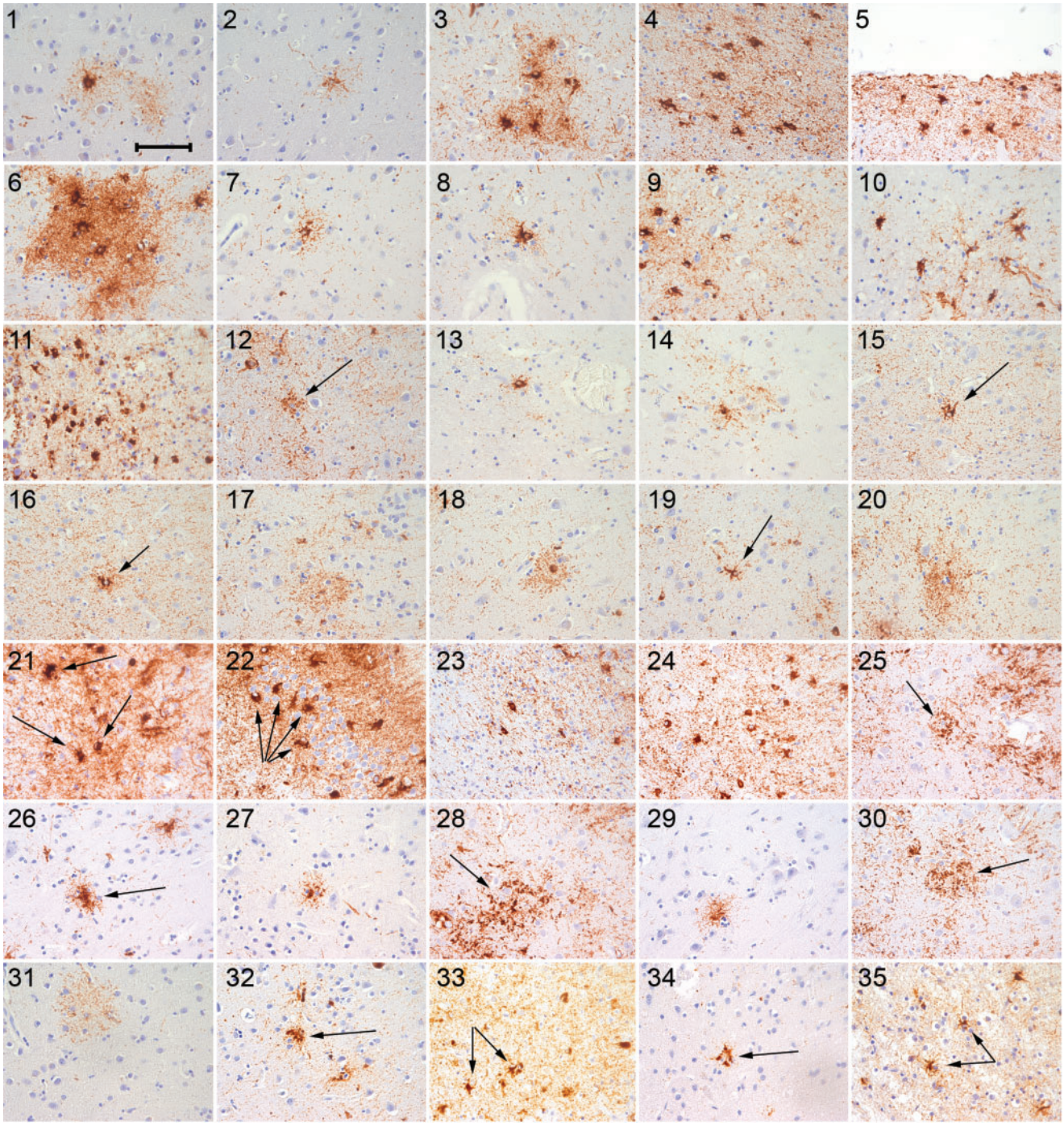

FIGURE 1. Microphotographs used in Study 1. The numbering corresponds to that listed in Table 3 with the consensus opinion. Arrows indicate the pathological astroglial tau immunoreactivities that were specifically evaluated. The bar in panel 1 represents 60 μm for all images.

(8). The "gold standard" was achieved by consensus of a reference group (G.G.K., J.Q.T., E.B.L., D.J.I., J.L.R., V.J., J.B.T., D.S.) who evaluated all images and scanned sections. This consensus meeting was held in the Department of Pathology and Laboratory Medicine, Center for Neurodegenerative Disease Research, Institute on Aging, University of Pennsylvania School of Medicine, Philadelphia, Pennsylvania. Only astrocytic pathology involving the whole cell body or cell processes but not isolated fine dots was accepted as pathological structures.

Statistical Analysis

The percentage (%) of agreement with a 95% confidence interval (CI) was calculated for each evaluation as well as the

TABLE 3. Reference Opinion and Interrater Agreement (% Agreement ± 95% Confidence Interval, CI) for the Microphotographs Note that these are not citations but the numbering of microphotographs Representing Astroglial Tau Immunoreactivities

Photo Nr.	Ref. Opinion Nr. 1	Interrater Agreement(%)	CI of %	Ref. Opinion Nr. 2	Interrater Agreement (%) Ref. 1+2	CI of %	2nd Most Frequent Opinion of the Evaluators	% of 2nd Most Frequent Opinion
1	GFA	97.78	±4.31	–	–	–	TA	2.22
2	GFA	73.33	±12.9	–	–	–	TA	11.1
3	GFA	62.22	±14.1	–	–	–	TSA	26.67
4	TSA	84.44	±10.5	–	–	–	GFA	4.44
5	TSA	91.11	±8.32	–	–	–	TA, RA, GFA	2.22
6	GFA	68.89	±13.5	TSA	86.67	±11.2	TSA	17.78
7	GFA	64.44	±13.9	–	–	–	RA	22.22
8	GFA	37.78	±14.1	–	–	–	TSA	37.78
9	TSA	75.56	±12.5	–	–	–	RA, GFA	6.67
10	TSA	64.44	±13.9	GFA	64.44	±13.9	RA	28.89
11	TSA	77.78	±12.1	–	–	–	GAI	11.11
12	GAI	42.22	±14.4	–	–	–	AP	37.78
13	TSA	80.00	±11.6	–	–	–	TA, GFA	11.11
14	GFA	60.00	±14.3	–	–	–	AP	26.67
15	RA	44.44	±14.5	TA	57.78	±14.4	TSA	24.44
16	TA	24.44	±12.5	RA	35.56	±13.9	GFA, TSA	24.44
17	AP	73.33	±12.9	–	–	–	GFA	13.33
18	GFA	68.89	±13.5	–	–	–	AP	15.56
19	GFA	6.67	±7.28	RA	28.89	±13.2	TSA	31.11
20	GFA	31.82	±13.6	AP	86.36	±10.0	AP	54.55
21	TSA	68.89	±13.5	–	–	–	GFA	15.56
22	TSA	73.33	±12.9	–	–	–	RA, GAI, GFA	6.67
23	TSA	57.78	±14.4	–	–	–	GAI	24.44
24	TSA	71.11	±13.2	–	–	–	GFA	15.56
25	AP	88.89	±9.19	–	–	–	GAI	6.67
26	TA	44.44	±14.5	–	–	–	RA	26.67
27	TA	62.22	±13.9	–	–	–	RA	24.44
28	AP	80.00	±11.1	–	–	–	Uncl	6.67
29	TA	68.89	±13.5	–	–	–	RA, Uncl	8.89
30	AP	88.89	±9.19	–	–	–	Uncl	4.44
31	GFA	40.00	±14.3	–	–	–	AP	40.00
32	GAI	91.11	±8.32	–	–	–	GFA	6.67
33	RA	8.89	±8.31	–	–	–	TSA	68.89
34	GAI	91.11	±8.32	–	–	–	Uncl, TSA, GFA, TA	2.22
35	RA	68.18	±13.6	–	–	–	TA	25.00

GAI, globular astrocytic inclusion; AP, astrocytic plaque; TA, tufted astrocyte; RA, ramified astrocyte; Uncl, unclassifiable astroglial tau immunoreactivity.

mean % of agreements. In addition, a weighted kappa value (24) was calculated to assess concordance between each rater's response and the reference consensus, resulting in 45 kappa values for each study. Then, the overall kappa value was generated by averaging the 45 kappa values, and the 95% CI generated using a bootstrap procedure. The bootstrap resampling method was performed by resampling cases 1000 times. The above process was performed for 10 different study questions (Table 2). When a kappa value could not be generated for a particular rater due to absence of variation in her/his responses for all subquestions in a given study, the Maxwell's random error coefficient of agreement (25) was applied as an alternative. Kappa value or Maxwell's statistic above 0.81 was considered almost perfect agreement, 0.61–0.80 as substantial, 0.41–0.60 as moderate, and 0.21–0.4 as fair agreement (26). Both kappa value and Maxwell statistic correct for random chance agreement, and thus they are generally lower than the % agreement, which does not correct for random chance of agreement.

RESULTS

Evaluation of Astrocytic Tau Immunoreactivity (Study 1)

The reference group defined the astrocytic morphology of tau pathologies on 35 images (Fig. 1; Table 3): 11 GFA, 10

TSA, 4 each of astrocytic plaques and tufted astrocytes, and 3 each of globular astroglial inclusions and ramified astrocytes. The group also provided a second option for 6 images (nos. 6, 10, 15, 16, 19, and 20; Table 3) as these images were open to debate. Forty-five evaluations were received. The agreement was above 60% for 35 images, including 9 out of 10 images of TSA, 7 out of 11 of GFA, 4 out of 4 of astrocytic plaques, 2 out of 4 of tufted astrocytes, 2 out of 3 of globular astroglial inclusions, and 1 out of 3 of ramified astrocytes. A lower agreement was reached for 1 out of 10 TSA, 4 out of 11 GFA, 2 out of 4 tufted astrocytes, 1 out of 3 globular astrocytic inclusions, and for 2 out of 3 ramified astrocytes.

Astrocytic plaques were interpreted by only a few observers as globular astroglial inclusions (GFA), or as unclassifiable astrocytic morphology. One image (no. 12) thought to be a globular astroglial inclusion was interpreted as an astrocytic plaque by 37.78% of the observers. This image was taken from the amygdala of an elderly individual showing no other neuropathological features of either GGT or CBD. Regarding this image, the reference group felt that the granular deposits had to be distinguished from the astrocytic plaque morphology. However, even the reference group noted that by looking at the image only, a globular morphology could be also suspected—and this was indeed the selection made by most of the observers. In further images GFA were mostly interpreted as astrocytic plaques or rarely as TSA or tufted astrocytes, whereas TSA were interpreted with the widest range of possible astrocytic morphologies (Table 3). Ramified astrocytes photographed from PiD cases were interpreted as TSA or tufted astrocytes by some of the evaluators. Finally, tufted astrocytes photographed from cases showing the neuropathological features of PSP, were interpreted as ramified astrocytes, GFA or TSA by a few observers. The mean % agreement were 82.8% for AP, 74.8% for GAI, 74.4% for TSA, 55.6% for GFA, 50.0% for tufted astrocytes, and 40.5% for ramified astrocytes, suggesting that ramified astrocytes, tufted astrocytes, and GFA may be more difficult to identify than the other pathologies. In summary, the overall % agreement for Study 1 was >60% with a value of 0.55 (95% CI 0.433–0.645; Table 2).

Recognition of ARTAG and Other Astroglial Tau Pathologies (Study 2A)

Forty-one evaluations were received. The evaluation of 25 scanned AT8-immunostained sections revealed high % agreement for the presence of ARTAG pathology (Table 4). In this series, 3 cases with neuropathological features of either PSP or CBD were included, and the lowest agreement was observed for these 3 cases. Scan 9 (Fig. 2A, B) represents the basal ganglia from a case showing ARTAG and early form of PSP (case 5; Table 1). While the presence of ARTAG was recognized by 68.29% of the observers, only 26.83% recognized tufted astrocytes in the section. Careful evaluation of the section revealed astrocytes compatible with GFA (Fig. 2A) and tufted astrocytes (Fig. 2B). Scan 16 (case 12; Table 1) shows the temporal cortex from a case with CBD (Fig. 2C, D) in which more than 50% of observers thought ARTAG to be also present. A section of the temporal cortex (scan 19; Fig. 2E, F) was evaluated from a case with PSP (case 13; Table 1); while ARTAG was recognized, only 52.5% agreed that tufted astrocytes could be seen as well. Finally, on scan 21 (case 21; Table 1), ~30% of the observers thought that the scan showed astrocytic plaques, but the consensus opinion was that only occasional GFA were present (Fig. 2G, H). Despite the high % agreement for the recognition of ARTAG and other astroglial tau pathologies associated with primary FTLD-tauopathies, kappa values were lower for these (0.48, 95% CI 0.457–0.900; and 0.25, 95% CI 2.89×10^{-16}, 0.374; respectively; Table 2).

TABLE 4. Interrater Agreement (% Agreement ±95% Confidence Interval, CI) for the Recognition of ARTAG and Other Astroglial Tau Pathologies

Scan	ARTAG	Agreement	95%CI	Other AG	Agreement	95%CI	No. of Evaluations
1	Yes	95.12	±6.59	No	78.05	±12.67	41
2	Yes	100.00	0	No	75.00	±13.42	40
3	Yes	100.00	0	No	80.00	±12.4	40
4	Yes	100.00	0	No	87.50	±10.25	40
5	Yes	100.00	0	No	82.50	±11.78	40
6	Yes	100.00	0	No	85.00	±11.07	40
7	Yes	80.00	±12.4	No	62.50	±15	40
8	Yes	100.00	0	No	75.00	±13.42	40
9	Yes	68.29	±14.24	TA	26.83	±13.56	41
10	Yes	92.68	±7.97	No	63.41	±14.74	41
11	Yes	100.00	0	No	80.49	±12.13	41
12	Yes	92.68	±7.97	No	87.80	±10.02	41
13	Yes	95.12	±8.45	No	80.49	±12.13	41
14	Yes	100.00	0	No	100.00	0	14
15	Yes	100.00	0	No	77.50	±12.94	40
16	No	48.78	±15.3	AP	63.41	±14.74	41
17	Yes	77.50	±12.94	No	60.00	±15.18	40
18	Yes	92.50	±8.16	No	77.50	±12.94	40
19	Yes	80.00	±12.4	TA	52.50	±15.48	40
20	Yes	100.00	0	No	95.00	±6.75	40
21	Yes	70.00	±14.2	No	67.50	±14.51	40
22	Yes	92.50	±8.16	No	47.50	±15.48	40
23	Yes	100.00	0	No	67.50	±14.51	40
24	Yes	97.50	±4.84	No	65.00	±14.78	40
25	Yes	95.00	±6.75	No	90.00	±9.3	40

Note that for case 14, only 14 evaluations were received due to technical reasons.

Recognition of ARTAG Types (Study 2A)

Next, we examined the agreement in the identification of different ARTAG types. For each subpial, subependymal, gray and white matter, and perivascular type of ARTAG, a high % agreement was reached (~80%), with kappa values (0.37–0.72) reflecting fair to substantial agreement (Table 2). Only a few examples can be listed for which considerable disagreement was observed (Table 5). In scans 3, 10, and 25, the reference group decided that the AT8-immunoreactive dots in subpial (Fig. 3A), subependymal (Fig. 3C), or perivascular

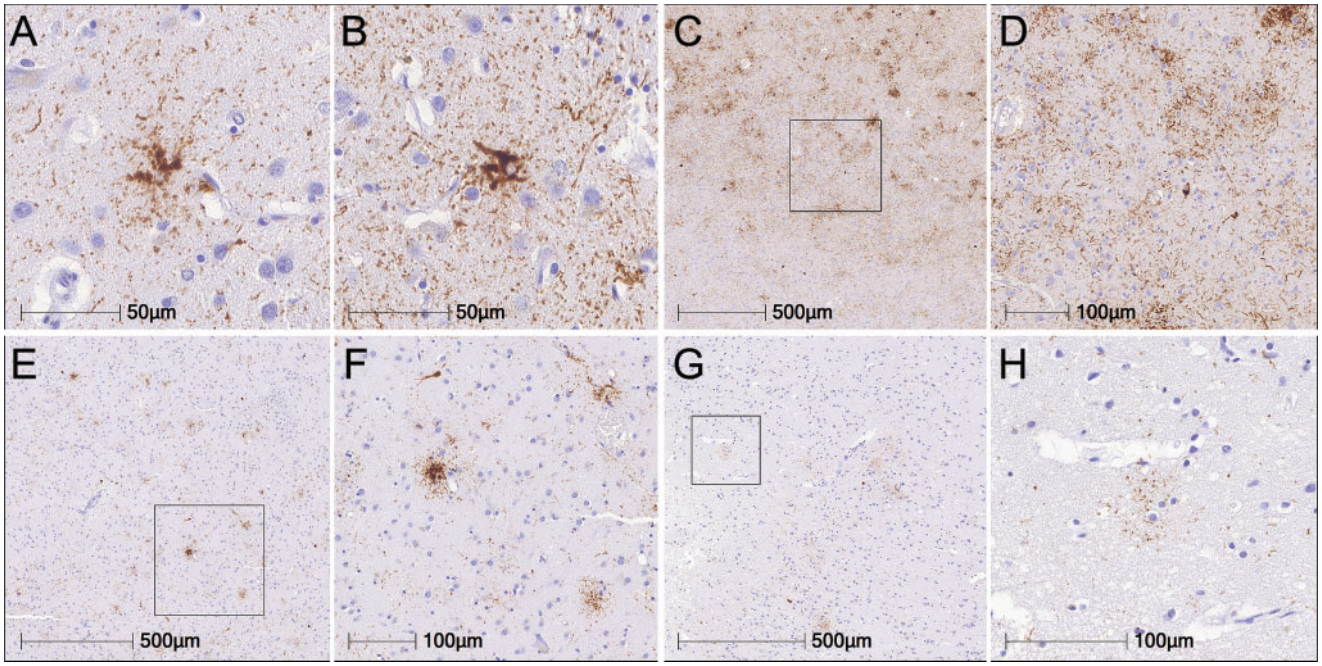

FIGURE 2. Representative images of pathological AT8-immunoreactive astrocytes in cases where the interrater agreement was lower than in others when the presence of ARTAG had to be decided. Granular/fuzzy astrocyte (**A**) and tufted astrocyte (**B**) in the striatum in scanned section 9 (case 5; PSP). Astrocytic plaques (**C**, **D**) in scanned section 16 (case 12; CBD). Astrocytic pathological tau immunoreactivities (**E**) in scanned section 19 with an early form of PSP (case 13) showing an example of a tufted astrocyte (upper left) and GFA (lower right, **F**). Occasional GFA in the temporal cortex in scanned section 21 (case 21) (**G**, **H**).

(Fig. 3E) locations were not sufficient to confirm ARTAG. However, occasional TSA, subpial in scan 13 (Fig. 3B), subependymal in scan 24 (Fig. 3D), and perivascular in scan 7 (Fig. 3F), and thick astrocytic processes were recognized and interpreted as ARTAG. In scan 17 the reference group did not interpret the tau immunoreactivity in the white matter as ARTAG, but as oligodendroglial coiled bodies (Fig. 4A, B). Conversely, in scan 20, the group interpreted the AT8-immunoreactivity in the white matter in the vicinity of the inferior horn of the lateral ventricle as white matter ARTAG (Fig. 4C, D). On scan 10, the reference group did not interpret the single astrocytic-like AT8-immunoreactivity (Fig. 4E) in the dentate gyrus as ARTAG, while in the CA4 field, similar immunoreactivities were interpreted as such, leading to disagreement (Table 5). On scan 13, TSA in the dentate gyrus were interpreted as ARTAG (Fig. 4F) with a high % level of agreement (80.49%). In scan 12, several neuritic plaque-related tau profiles were observed in the inferior temporal gyrus (Fig. 4G), and due to lack of clear-cut characteristics of GFA or TSA, were not interpreted as ARTAG. In the temporal cortex (scan 15), occasional GFA (Fig. 4H) were interpreted as ARTAG with high % agreement (72.5%; Table 5). Finally, in scan 12, ARTAG was seen in both the hippocampal dentate gyrus (Fig. 4I) and the CA4 field (Fig. 4J), yet with variable % agreement among raters (87.8% vs 70.73%).

Evaluation of the Severity and Extent of ARTAG (Study 2B)

In all scans where ARTAG was observed, the reference group scored severity/extent in 90 locations. Concordance for these 90 locations ranged from 12.5% to 87.5% (mean 50.49%) with a kappa value of 0.39 ± 0.049 (Table 2). Next, we evaluated the agreement to decide whether the amount of tau-immunoreactive astrocytes and the extent of immunoreactivity is occasional or numerous, without further stratification of numerous for focally accentuated or widespread. For this parameter the % agreement was better (ranging from 22.5% to 100%) with a mean agreement of 65.9% (Table 2).

Finally, the overall assessment of ARTAG pathologies (all aforementioned aspects calculated) revealed 82.3% of agreement and a kappa value of 0.60 (95% CI 0.534–0.653) (Table 2).

DISCUSSION

The goal of this study was to evaluate the variation in the neuropathological assessment of ARTAG and other astrocytic tau immunoreactivities in single areas of various cases. While several studies have been conducted to determine interrater variability of AD-related neuropathological changes or Lewy body pathologies (3, 13), there is a paucity of data on consensus in the description and interpretation of pathological astrocytic tau immunoreactivities. Tufted astrocytes and astrocytic plaques are hallmark lesions of PSP and CBD (18), respectively, but the spectrum of astrocytic tau-immunoreactive morphologies extends beyond these 2 entities, even in PSP and CBD. Some of these morphologies are thought to represent early forms of tufted astrocytes (27), analogous to the concept of pretangles in neurons preceding neurofibrillary tangles (28). Further astrocytic morphologies have been de-

TABLE 5. Interrater Agreements (AGR; % Agreement ±95% Confidence Interval, CI) for Different ARTAG Types

Scan NrSP-SE-PV	SP	AGR	95%CI	SE	AGR	95%CI	PV	AGR	95%CI	Scan Nr WM	Region	WM	AGR	95%CI	Scan Nr GM	Region	GM	AGR	95%CI
1	No	92.68	±7.97	No	100.00	±0	No	95.12	±6.59	1	TEM	No	53.66	±15.2	1	TEM	Yes	92.68	±7.97
2	Yes	95.00	±6.75	No	100.00	0	Yes	80.00	±12.4	2	TEM	Yes	97.50	±4.84	2	TEM	Yes	97.50	±4.84
3	No	27.50	±13.8	No	75.00	±13.4	Yes	60.00	±15.1	3	FRO	Yes	92.50	±8.1	3	FRO	Yes	100.00	0
4	Yes	90.00	±9.3	Yes	70.00	±14.2	Yes	92.50	±8.16	4	IC	Yes	77.50	±12.9	4	CAUD	Yes	100.00	0
5	Yes	97.50	±4.84	Yes	100.00	0	Yes	97.50	±4.84	4	FRB	Yes	100.00	0	4	ACC	Yes	100.00	0
6	Yes	100.00	0	Yes	95.00	±6.75	Yes	97.50	±4.84	5	MES	Yes	92.50	±8.1	4	FRB	Yes	100.00	0
7	Yes	72.50	±13.8	No	72.50	±13.8	Yes	37.50	±15.0	6	MED-MID	Yes	97.50	±4.8	5	MES	Yes	97.50	±4.84
8	Yes	95.00	±6.75	Yes	100.00	0	Yes	92.50	±8.16	6	PYR	Yes	100.00	0	6	HYPOG	Yes	100.00	0
9	No	95.12	±6.59	No	97.56	±4.72	No	78.05	±12.6	7	AMY	Yes	72.50	±13.8	7	AMY	Yes	75.00	±13.4
10	Yes	73.17	±13.5	No	51.22	±15.3	No	75.61	±13.1	8	AMY	Yes	95.00	±6.75	8	AMY	Yes	100.00	0
11	Yes	92.68	7±.97	No	78.05	±12.7	Yes	58.54	±15.0	9	IC	No	73.17	±13.5	9	CAUD	Yes	65.85	±14.5
12	Yes	82.93	±11.2	Yes	65.85	±14.5	Yes	56.10	±15.1	10	TEM	No	78.05	±12.6	10	CA1–4	Yes	58.54	±15.0
13	Yes	70.73	±13.9	Yes	90.24	±9.08	Yes	56.10	±15.1	11	AMY	Yes	68.29	±14.2	10	DG	No	51.22	±15.3
14	No	85.71	±10.8	No	100.00	0	Yes	64.29	±14.8	12	TEM	Yes	92.68	±7.97	10	TEM	Yes	82.93	±11.5
15	Yes	100.00	0	No	57.50	±15.3	Yes	82.50	±11.7	13	TEM	Yes	92.68	±7.97	11	AMY	Yes	85.37	±10.8
16	No	58.54	±15.0	No	95.12	6.59	No	85.37	±10.8	14	TEM	Yes	100.00	0	11	GYAMB	Yes	80.49	±12.1
17	No	90.00	±9.3	No	100.00	0	No	90.00	±9.3	15	TEM	Yes	97.50	±4.84	12	CA1–4	Yes	70.73	±13.9
18	No	60.00	±15.1	No	92.50	±8.16	No	75.00	±13.4	16	TEM	No	63.41	±14.7	12	DG	Yes	87.80	±10.0
19	No	70.00	±14.2	No	100.00	0	No	95.00	±6.75	17	FRO	No	42.50	±15.3	12	TEM	No	34.15	±14.5
20	Yes	100.00	0	Yes	95.00	±6.75	Yes	65.00	±14.7	18	CING	Yes	87.50	±10.2	13	CA1–4	No	43.90	±15.1
21	No	77.50	±12.9	No	100.00	0	No	97.50	±4.84	19	TEM	Yes	65.00	±14.7	13	DG	Yes	80.49	±12.1
22	No	92.50	±8.16	No	100.00	0	No	97.50	±4.84	20	TEM	No	55.00	±15.4	13	TEM	Yes	78.05	±12.6
23	No	56.41	±15.5	No	84.62	±11.3	No	76.92	±13.2	20	HIPP	Yes	87.50	±10.2	14	CA1–4	No	85.71	±10.8
24	Yes	97.50	±4.84	Yes	70.00	±14.2	Yes	75.00	±13.4	21	TEM	No	82.50	±11.7	14	DG	No	92.86	±7.98
25	Yes	72.50	±13.8	No	90.00	±9.3	No	72.50	±13.8	22	FRO	Yes	62.50	±15.0	14	TEM	No	64.29	±14.8
										23	IC	No	58.97	±15.4	15	CA1–4	Yes	87.50	±10.2
										23	FRB	Yes	92.31	±8.36	15	DG	Yes	92.50	±8.16
										24	IC	No	72.50	±13.8	15	TEM	Yes	72.50	±13.8
										24	FRB	Yes	92.50	±8.16	16	TEM	No	63.41	±14.7
										25	MES	No	42.50	±15.3	17	FRO	Yes	77.50	±12.9
															18	CING	Yes	90.00	±9.3
															19	TEM	Yes	80.00	±12.4
															20	CA1–4	Yes	85.00	±11.0
															20	DG	Yes	100.00	0
															20	TEM	Yes	92.50	±8.16
															21	TEM	Yes	67.50	±14.5
															22	FRO	Yes	92.50	±8.16
															23	CAUD	Yes	94.87	±6.92

(continued)

TABLE 5 Continued

Scan NrSP-SE-PV	SP AGR	95%CI	SE AGR	95%CI	PV AGR	95%CI	Scan Nr WM	Region	WM AGR	95%CI	Scan Nr GM	Region	GM	AGR	95%CI
											23	ACC	Yes	89.74	±9.52
											23	FRB	Yes	87.18	±10.4
											24	CAUD	Yes	92.50	±8.16
											24	ACC	Yes	85.00	±11.0
											24	FRB	Yes	90.00	±9.3
											25	MES	Yes	95.00	±6.75

GM, gray matter; PV, perivascular; SE, subependymal; SP, subpial; WM, white matter) in different anatomical regions (ACC, nucleus accumbens; AMY, amygdala; CA1–4, cornu ammonis 1–4 fields; CAUD, caudate nucleus; CING, anterior cingulate cortex; DG, dentate gyrus; FRO, frontal cortex; FRB, frontobasal, including gyrus rectus and orbital gyri; GYAMB, gyrus ambiens; HYPOG, hypoglossal nucleus; IC, internal capsule; MES, mesencephalon; MED-MID, medulla oblongata midline; PYR, pyramid; TEM, temporal.

scribed in primary FTLD-Tau, such as the ramified astrocytes in PiD (21) and globular astrocytic inclusions in GGT (20). The recent consensus statement on the evaluation of ARTAG aimed to harmonize the description of pathological astrocytic tau morphologies and added GFA and TSA to this spectrum of pathological tau immunoreactivities (8). Our study revealed that the overall assessment of ARTAG shows a moderate agreement (kappa: 0.59, 95% CI 0.534–0.653) among raters across multiple international centers. In several evaluations we observed considerable discrepancy between the % agreement and the calculated kappa values. This is because kappa value corrects for random chance agreement, while the % agreement does not. Therefore, the % agreement overestimates the true probability that raters will answer a given question correctly when they are not just guessing. This is why the kappa values are consistently lower; it is by design. Thus, kappa value is a more conservative summary measure than the % agreement. It must be noted that kappa value could not be calculated for each image or case separately because there is only one reference opinion for these. Instead, each kappa value quantifies the agreement of each rater with the reference opinion on all cases, corrected for the probability that the rater might have blindly guessed.

To include researchers and neuropathologists from all over the world, we decided to use the cost-effective method of digital pathology, which is broadly applied for diagnostic purposes, including postmortem neuropathologic evaluations (3). Our first study focused on images of single astrocytic pathological tau immunoreactivities, and the second on the evaluation of scanned slides. We are aware that evaluating single images and scans of circumscribed anatomical regions may have accounted for a proportion of the disagreement observed (i.e. neuropathological evaluation requires the evaluation of several anatomical regions). We cannot exclude that the conservative results achieved by evaluating simple static pictures even with digital scanners would considerably improve with real microscoping. In a recent study on multisite assessment of NIA-AA criteria of AD-related pathologies, whole-slide images decreased the performance for the evaluation of severity and scores of amyloid-μ plaques (3). On the other hand, with this approach we were able to eliminate bias during the evaluation of cases in the current study. This means, for example, that if an observer looked across many anatomical regions and decided that the diagnosis is PSP or CBD, then the spectrum of pathological tau astrocytic morphologies may be overlooked or not described in detail, with most classified as tufted astrocytes or astrocytic plaques. Evaluating only a small number of anatomical regions or brain biopsies for the diagnosis of neurodegenerative diseases could potentially lead to misinterpretation in the classification of astrocytic tau pathologies. We noted variability in the evaluation of ramified astrocytes, which tended to be underrecognized. Conversely, in some cases, TSAs and tufted astrocytes were misinterpreted as these ramified morphologies. This might be due to the fact that PiD is a rare disorder, which shows variability in the presence and severity of pathological astrocytic tau immunoreactivity (21, 29, 30). Indeed, ramified astrocytes are amongst the less studied of the pathological tau astrocytic morphologies. Although we cannot exclude the possibility that ramified astrocytes are

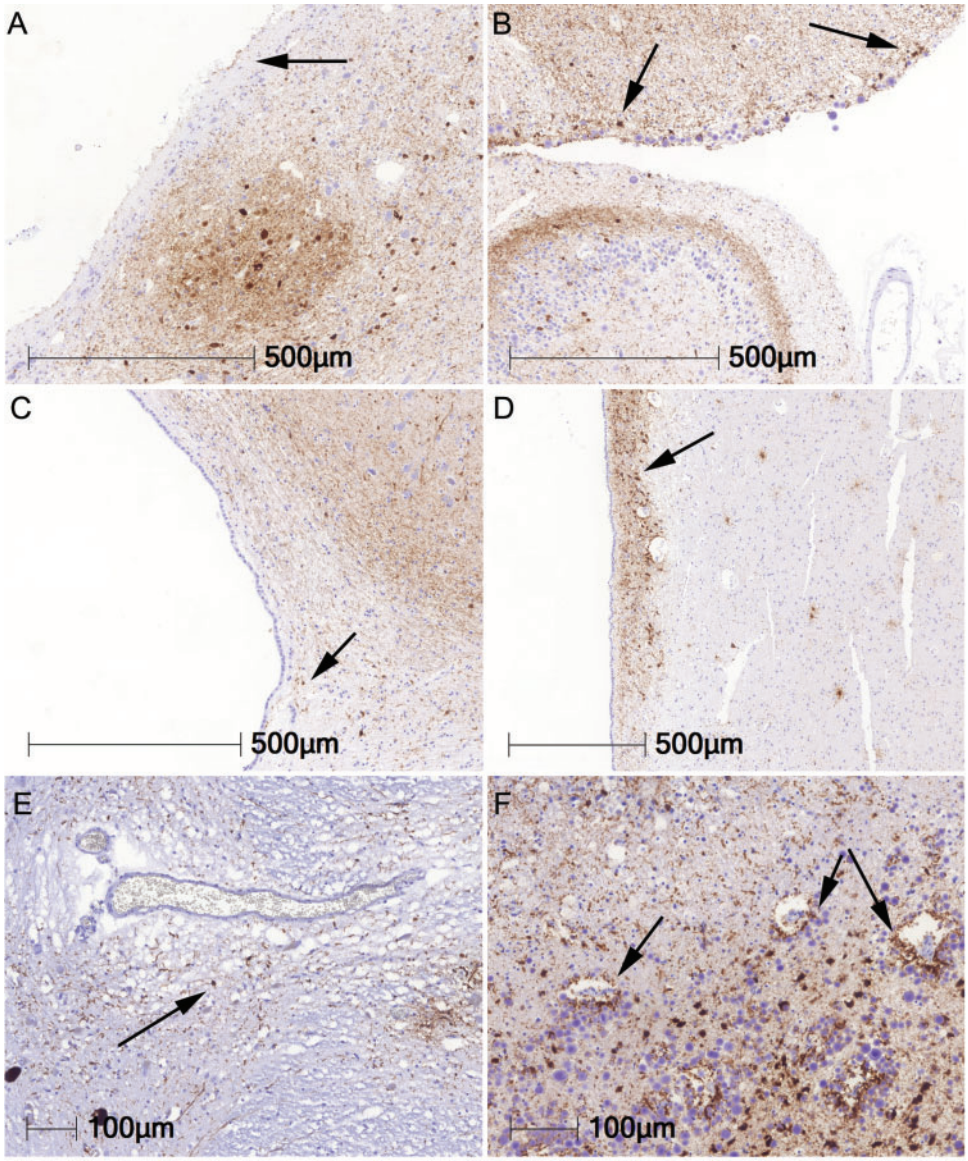

FIGURE 3. Representative photomicrographs of different ARTAG types for which discrepancy was observed between the consensus opinion and the observers (see also Table 4). In scans 3, 10, and 25 the reference group did not interpret the fine dots (arrows) as subpial (**A**), subependymal (**C**), or perivascular (**E**) ARTAG, respectively. In cases 13, 24, and 7 thorny astrocytes and thick astrocytic processes (arrows) were interpreted as subpial (**B**), subependymal (**D**), and perivascular (**F**) ARTAG, respectively.

present in the aging brain without the neuronal tau pathology characteristic of PiD, these astrocytes frequently show 3R tau isoform immunoreactivity in PiD (22, 30), which might represent a useful tool to reconcile these discrepancies. Some difficulty was also observed for the recognition of individual TSA in microphotographs. This was not a problem for scanned sections when, depending on the location (i.e. subpial, subependymal, perivascular), even without the classical thorny appearance, astrocytes were interpreted as ARTAG. However, when single astrocytic tau morphologies are evaluated in these locations, the TSA-like appearance may not be recognized.

The recognition of subependymal, subpial, and perivascular ARTAG showed high % agreement. However, cases with infrequent tau-immunoreactivity in these regions contributed to differences in interrater interpretation (see also low concordance for the evaluation of severity). On the other hand, recognition of white and gray matter ARTAG revealed less concordance between raters. For the white matter this was mostly due to scans with occasional TSA in the white matter or with the additional accumulation of oligodendroglial tau-immunoreactivity. For the gray matter, recognition of GFA posed some difficulties when only occasional GFA were seen, or in cases with neuropathological features of primary FTLD-

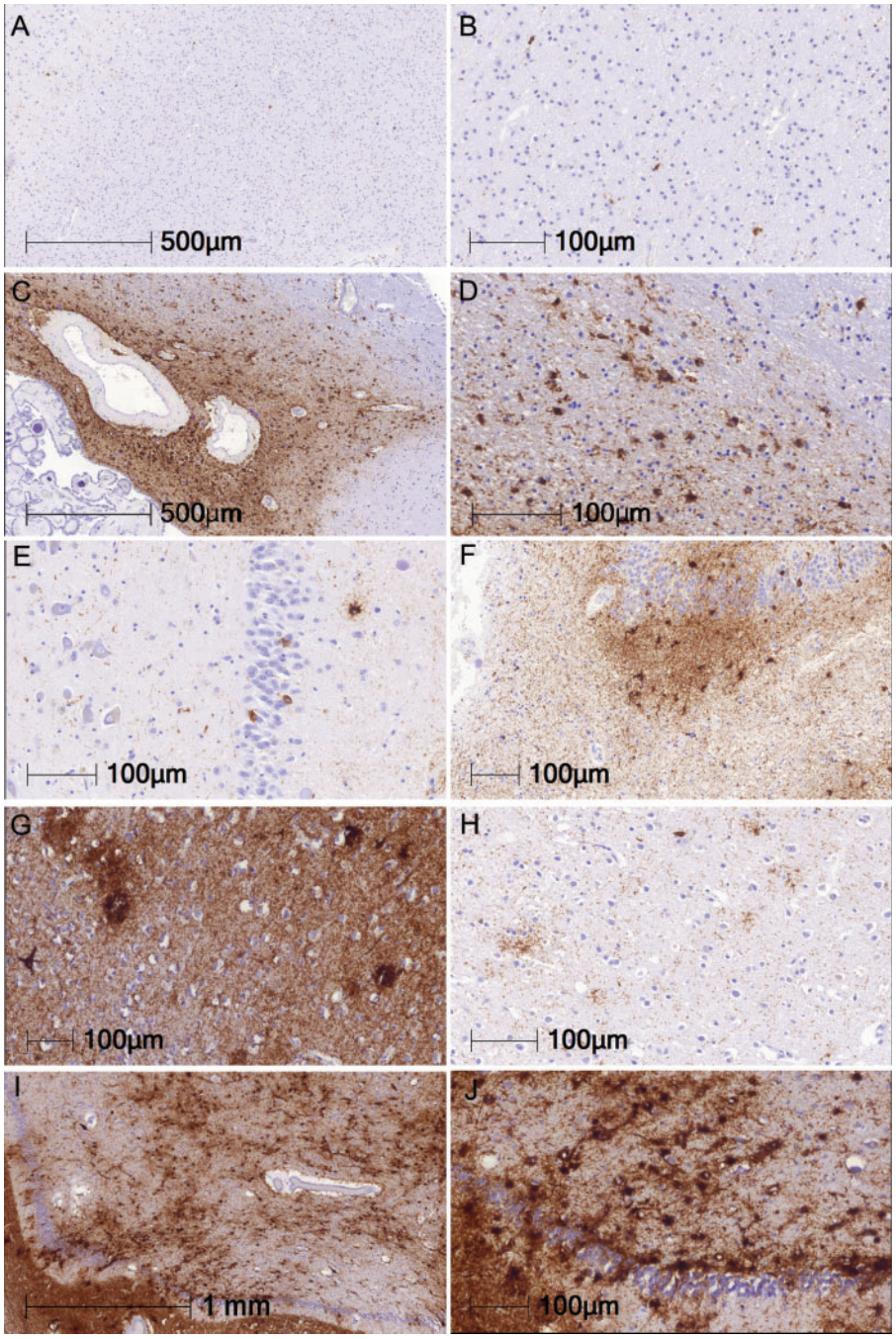

FIGURE 4. Representative images of different ARTAG types for which discrepancy was observed between the reference group and the observers (see also Table 4). In scan 17, the reference group did not interpret the AT8-immunoreactivity in the white matter as ARTAG but as oligodendroglial coiled bodies (**A**; enlarged in **B**). In scan 20, the reference group interpreted the AT8 immunoreactivity in the white matter in the vicinity of the inferior ventricle as white matter ARTAG (**C**, **D**). In scan 10, the reference group did not interpret the single astrocytic-like AT8 immunoreactivity (**E**; arrow) as ARTAG. In scan 13, thorny astrocytes in the dentate gyrus were interpreted as ARTAG (**F**). Neuritic plaque tau profiles in the temporal cortex (**G**) that were not interpreted as ARTAG in case 12. In the temporal cortex of case 15, occasional GFA (**H**) were interpreted as ARTAG. In scan 12, ARTAG was seen in both the dentate gyrus (**I**) and the CA4 field (**J**) but with variable levels of agreement.

tauopathies. Indeed, our study (in particular Study 2A) demonstrated that GFA morphologies in the gray matter occur in both PSP and CBD, suggesting a pathogenic relationship to the AT8-immunoreactive lesions seen in primary FTLD-Tau disorders. Importantly, several cases included in this study in which some observers suspected primary FTLD-Tau-related

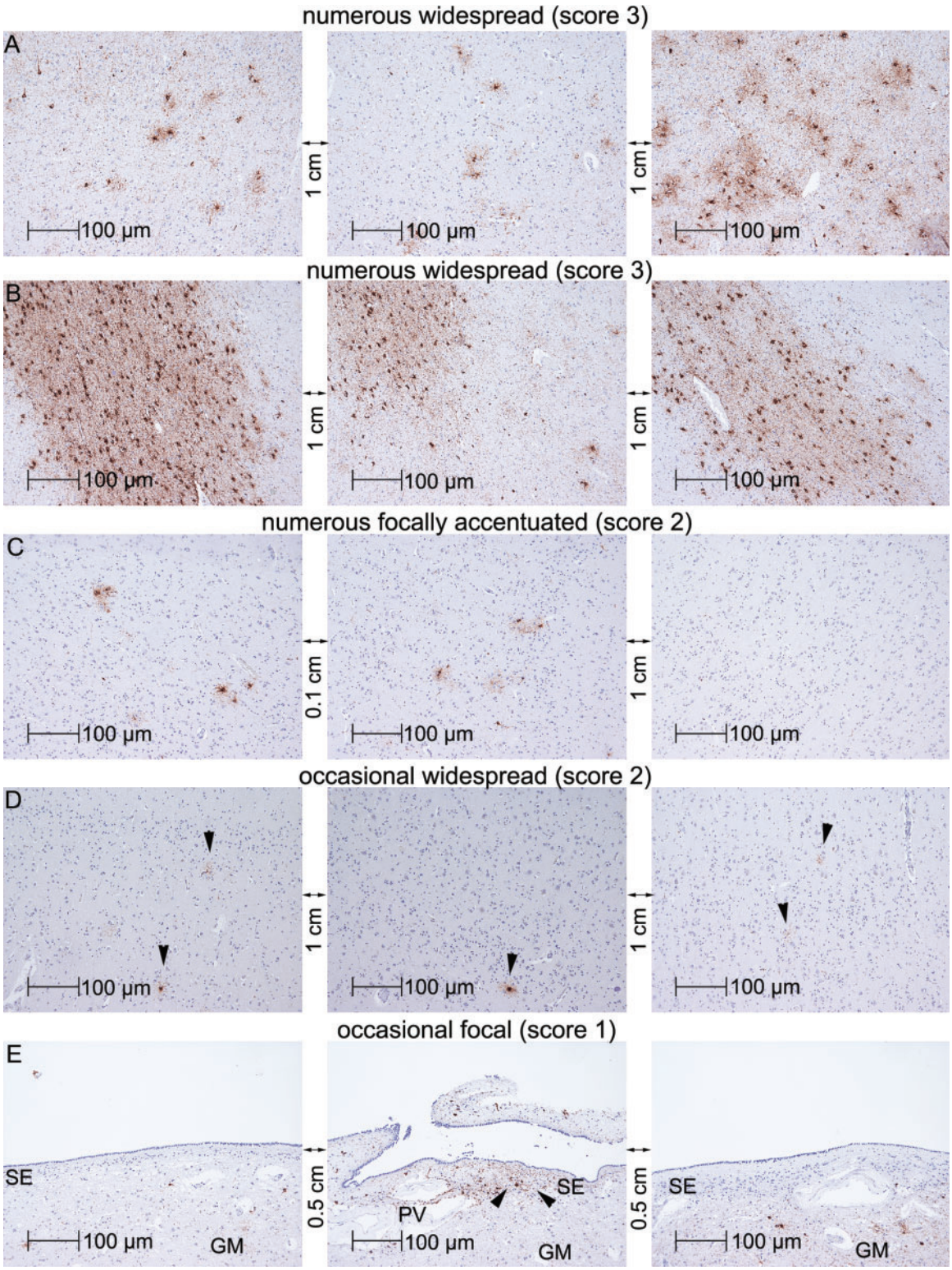

FIGURE 5. Representative images of the scoring strategy (**A**, **C**, **D**: gray matter; **B**: white matter; **E**: subependymal ARTAG)." Occasional" immunoreactivities are indicated by arrowheads. Abbreviations: SE, subependymal; GM, gray matter; PV, perivascular.

astrocytic tau pathologies occurred in cases older than 85 years of age. It is noteworthy that GFA were often identified as astrocytic plaques by evaluators (4 of 11 GFA), and that astrocytic plaques as the second most frequent opinion by evaluators predominated in the assessment of GFA. These findings suggest that the spatial arrangement pattern of tau accumulation in GFAs can resemble that of astrocytic plaques. In fact, based on the evaluation of ARTAG in a large cohort of cases we suggested the concept that the progression pattern of tau accumulation in the cytoplasm and processes of astrocytes associated with GFA or astrocytic plaques or tufted astrocytes shows common steps (31). Based on a comprehensive study on AGD and PSP cases, a similar concept was presented recently by Ikeda et al. Specifically, they suggested that at least some GFA-like morphologies (termed tufted astrocyte-like astrocytic lesions in that study) can potentially evolve into Gallyas-positive tufted astrocytes in AGD brains (32). Further studies are needed to clarify the relationship between gray matter ARTAG and GFA-like AT8-immunoreactivities in primary FTLD-tauopathy brains.

The lowest concordance was observed for the evaluation of severity and extent of ARTAG. While the distinction between occasional and numerous was easily made, several aspects remained problematic. For the original recommendation for the description of ARTAG severity, instead of the commonly used three-tiered semiquantitative strategy (mild, moderate, severe) we aimed to distinguish between the focal accumulation of ARTAG astrocytes (e.g. subpial TSA in cortical areas in the depths of sulci) and a more widespread distribution – in the gray matter as GFA or in the white matter as TSA. Many evaluators expressed difficulty assessing whether single-appearing (i.e. on a birds-eye view), AT8-immunoreactive astrocytes ought to be interpreted as occasional or numerous/widespread as required by the original scoring system (8) when they occurred along the cortical ribbon with a 500–2000 μm distance between them. The way one had to manipulate the digital slides, such as zooming in and out, may have also contributed to the discordance in determining the amount of ARTAG. It is a challenge to incorporate the different distribution patterns of ARTAG into a simple scoring system, especially considering that morphometric methods that distinguish between neuronal and astrocytic tau immunoreactivities are not available.

In view of the present findings, we recommend the following strategy (Fig. 5) with modest changes (i.e. adding a further group for occasional) to the proposals in the original ARTAG consensus harmonization paper (8): i) After the recognition of the morphology of pathological astrocytic tau immunoreactivity at high magnification (200–400×), the extent of involvement in a selected anatomical area should be evaluated at low magnification (50–100×); ii) If occasional pathological tau-immunoreactive astrocytes appear in a circumscribed area of a specific anatomical region, it should be designated as "occasional and focal" (score 1, corresponding to mild in a semiquantitative evaluation approach); iii) If occasional pathological tau-immunoreactive astrocytes are scattered throughout an anatomical region, the severity/extent should be designated as "occasional widespread" (score 2, corresponding to moderate in a semiquantitative evaluation approach); iv) If numerous pathological tau-immunoreactive astrocytes appear in a circumscribed area of a specific anatomical region, it should be designated as "numerous, focally accentuated" (score 2, corresponding to moderate in a semiquantitative evaluation approach); and v) If numerous pathological tau-immunoreactive astrocytes appear throughout an anatomical region, it should be designated as "numerous, widespread" (score 3, corresponding to severe in a semiquantitative evaluation approach).

In summary, we found that the application of a harmonized consensus evaluation strategy for the description of ARTAG (8) yields a moderate interrater concordance between neuropathologists at different centers. Improvement is needed in evaluations of the severity and extent of ARTAG types. Our study suggests that the spectrum of coexisting pathological astrocytic tau immunoreactivities may be wider than generally assumed in primary FTLD-Tau disorders if more care is taken to describe these lesions. This concept does not weaken the diagnostic importance of pathological tau positive tufted astrocytes, astrocytic plaques, ramified astrocytes and globular astrocytic inclusions as specific morphologies associated with certain primary FTLD-Tau disorders. In addition, this notion might help our understanding of the pathogenic relevance of ARTAG and its relation to primary FTLD-Tau and other diseases with astrocytic tau pathology such as chronic traumatic encephalopathy (33). Overall, our study supports the application of the current harmonized consensus evaluation strategy of ARTAG (8) with slight modifications in the evaluation of its severity and extent. Agreement can be increased by consensus meetings including a joint assessment of cases (10), teaching courses, but also by utilizing image analysis techniques for the identification of the specific tau immunoreactive patterns, density in different locations. This will facilitate further worldwide collection and comparison of data on ARTAG for research purposes. Our study revealed, however, the challenging issue of always readily differentiating and clearly classifying tau-positive astrocytic lesions. It should also motivate further exploration of the significance of astrocytic lesions in neurodegenerative disorders.

REFERENCES

1. Toledo JB, Brettschneider J, Grossman M, et al. CSF biomarkers cutoffs: the importance of coincident neuropathological diseases. Acta Neuropathol 2012;124:23–35
2. Montine TJ, Phelps CH, Beach TG, et al. National institute on aging-Alzheimer's association guidelines for the neuropathologic assessment of Alzheimer's disease: a practical approach. Acta Neuropathol 2012; 123:1–11
3. Montine TJ, Monsell SE, Beach TG, et al. Multisite assessment of NIA-AA guidelines for the neuropathologic evaluation of Alzheimer's disease. Alzheimer's Dement 2016;12:164–9
4. Crary JF, Trojanowski JQ, Schneider JA, et al. Primary age-related tauopathy (PART): a common pathology associated with human aging. Acta Neuropathol 2014;128:755–66
5. Lace G, Ince PG, Brayne C, et al. Mesial temporal astrocyte tau pathology in the MRC-CFAS ageing brain cohort. Dement Geriatr Cogn Disord 2012;34:15–24
6. Schultz C, Ghebremedhin E, Del Tredici K, et al. High prevalence of thorn-shaped astrocytes in the aged human medial temporal lobe. Neurobiol Aging 2004;25:397–405
7. Kovacs GG, Milenkovic I, Wohrer A, et al. Non-Alzheimer neurodegenerative pathologies and their combinations are more frequent than commonly believed in the elderly brain: a community-based autopsy series. Acta Neuropathol 2013;126:365–84

8. Kovacs GG, Ferrer I, Grinberg LT, et al. Aging-related tau astrogliopathy (ARTAG): harmonized evaluation strategy. Acta Neuropathol 2016;131: 87–102
9. Alafuzoff I, Pikkarainen M, Al-Sarraj S, et al. Interlaboratory comparison of assessments of Alzheimer disease-related lesions: a study of the BrainNet Europe Consortium. J Neuropathol Exp Neurol 2006;65: 740–57
10. Alafuzoff I, Arzberger T, Al-Sarraj S, et al. Staging of neurofibrillary pathology in Alzheimer's disease: a study of the BrainNet Europe Consortium. Brain Pathol 2008;18:484–96
11. Alafuzoff I, Parkkinen L, Al-Sarraj S, et al. Assessment of alpha-synuclein pathology: a study of the BrainNet Europe Consortium. J Neuropathol Exp Neurol 2008;67:125–43
12. Alafuzoff I, Pikkarainen M, Arzberger T, et al. Inter-laboratory comparison of neuropathological assessments of beta-amyloid protein: a study of the BrainNet Europe consortium. Acta Neuropathol 2008;115:533–46
13. Alafuzoff I, Ince PG, Arzberger T, et al. Staging/typing of Lewy body related alpha-synuclein pathology: a study of the BrainNet Europe Consortium. Acta Neuropathol 2009;117:635–52
14. Alafuzoff I, Thal DR, Arzberger T, et al. Assessment of beta-amyloid deposits in human brain: a study of the BrainNet Europe Consortium. Acta Neuropathol 2009;117:309–20
15. Irwin DJ, Cairns NJ, Grossman M, et al. Frontotemporal lobar degeneration: defining phenotypic diversity through personalized medicine. Acta Neuropathol 2015;129:469–91
16. Kovacs GG. Invited review: neuropathology of tauopathies: principles and practice. Neuropathol Appl Neurobiol 2015;41:3–23
17. Hauw JJ, Daniel SE, Dickson D, et al. Preliminary NINDS neuropathologic criteria for Steele–Richardson–Olszewski syndrome (progressive supranuclear palsy). Neurology 1994;44:2015–9
18. Dickson DW. Neuropathologic differentiation of progressive supranuclear palsy and corticobasal degeneration. J Neurol 1999;246 Suppl 2: II6–15
19. Dickson DW, Bergeron C, Chin SS, et al. Office of rare diseases neuropathologic criteria for corticobasal degeneration. J Neuropathol Exp Neurol 2002;61:935–46
20. Ahmed Z, Bigio EH, Budka H, et al. Globular glial tauopathies (GGT): consensus recommendations. Acta Neuropathol 2013;126:537–44
21. Dickson DW. Pick's disease: a modern approach. Brain Pathol 1998;8: 339–54
22. Ferrer I, Lopez-Gonzalez I, Carmona M, et al. Glial and neuronal tau pathology in tauopathies: characterization of disease-specific phenotypes and tau pathology progression. J Neuropathol Exp Neurol 2014;73:81–97
23. Botez G, Probst A, Ipsen S, et al. Astrocytes expressing hyperphosphorylated tau protein without glial fibrillary tangles in argyrophilic grain disease. Acta Neuropathol 1999;98:251–6
24. Cohen J. Weighted kappa: nominal scale agreement with provision for scaled disagreement or partial credit. Psychol Bull 1968;70:213–20
25. Maxwell AE. Coefficients of agreement between observers and their interpretation. Br J Psychiatry 1977;130:79–83
26. Landis JR, Koch GG. The measurement of observer agreement for categorical data. Biometrics 1977;33:159–74
27. Santpere G, Ferrer I. Delineation of early changes in cases with progressive supranuclear palsy-like pathology. Astrocytes in striatum are primary targets of tau phosphorylation and GFAP oxidation. Brain Pathol 2009;19:177–87
28. Bancher C, Brunner C, Lassmann H, et al. Accumulation of abnormally phosphorylated tau precedes the formation of neurofibrillary tangles in Alzheimer's disease. Brain Res 1989;477:90–9
29. Irwin DJ, Brettschneider J, McMillan CT, et al. Deep clinical and neuropathological phenotyping of Pick disease. Ann Neurol 2016;79:272–87
30. Kovacs GG, Rozemuller AJ, van Swieten JC, et al. Neuropathology of the hippocampus in FTLD-Tau with Pick bodies: a study of the BrainNet Europe Consortium. Neuropathol Appl Neurobiol 2013;39:166–78
31. Kovacs GG, Robinson JL, Xie SX, et al. Evaluating the patterns of aging-related tau astrogliopathy (ARTAG) unravels novel insights into brain-aging and neurodegenerative diseases. J Neuropathol Exp Neurol 2017;76:270–88
32. Ikeda C, Yokota O, Nagao S, et al. The relationship between development of neuronal and astrocytic tau pathologies in subcortical nuclei and progression of argyrophilic grain disease. Brain Pathol 2016;26:488–505
33. McKee AC, Cairns NJ, Dickson DW, et al. The first NINDS/NIBIB consensus meeting to define neuropathological criteria for the diagnosis of chronic traumatic encephalopathy. Acta Neuropathol 2016;131:75–86
34. Braak H, Alafuzoff I, Arzberger T, et al. Staging of Alzheimer disease-associated neurofibrillary pathology using paraffin sections and immunocytochemistry. Acta Neuropathol 2006;112:389–404
35. Thal DR, Rub U, Orantes M, et al. Phases of A beta-deposition in the human brain and its relevance for the development of AD. Neurology 2002; 58:1791–800